Bubble-Column and Airlift Photobioreactors for Algal Culture

Asterio Sánchez Mirón, Francisco García Camacho, Antonio Contreras Gómez, Emilio Molina Grima, and Yusuf Chisti
Dept. of Chemical Engineering, University of Almería, E-04071 Almería, Spain

Bubble columns and airlift photobioreactors can be useful for culturing phototrophic organisms requiring light as a nutrient. Light availability in bubble columns and airlift devices is influenced by aeration rate, gas holdup, and the liquid velocity (mixing and turbulence). The photosynthetically generated oxygen also needs to be removed, as excessive dissolved oxygen suppresses photosynthesis. Oxygen removal capacity is governed by the magnitude of the overall gas–liquid mass-transfer coefficient, $k_L a_L$. This work characterizes the relevant hydrodynamic and mass-transfer parameters in three air-agitated reactors: bubble column, split-cylinder airlift device and concentric draft-tube sparged airlift vessel. The reactors are then evaluated for culture of the microalga Phaeodactylum tricornutum. All reactors were about 0.06 m^3 in working volume, and the working aspect ratio was about 10. Data were obtained in tap water for a base-line comparison and in Mediterranean seawater, as a potential medium for algal culture. A theoretical relationship was developed and proved between $k_L a_L$ and the aeration rate. In addition, a method based on mechanistic relationships was proved for predicting the liquid circulation velocity and $k_L a_L$ in airlift reactors. Existing correlations applied satisfactorily to gas holdup and $k_L a_L$ data obtained in the bubble column. Aqueous solution of sodium chloride (0.15 M) closely resembled seawater in terms of its hydrodynamics and oxygen transfer behavior. Under the conditions tested, all three reactors attained a biomass concentration of about 4 $kg \cdot m^{-3}$ after ~ 260 h. The mean maximum specific growth rate was 0.022 h^{-1} in all cases at a power input of 109 $W \cdot m^{-3}$.

Introduction

Airlift and bubble-column bioreactors are simple devices that have gained wide acceptance in gas–liquid contacting applications in bioprocessing, the chemical process industry, and treatment of wastewater. Substantial knowledge exists on gas–liquid hydrodynamics and mass transfer in bubble columns and airlift bioreactors, as comprehensively discussed in major treatise (Chisti and Moo-Young, 1987; Chisti, 1989, 1998, 1999a, b; Deckwer, 1992; Joshi et al., 1990; Merchuk and Gluz, 1999). With few exceptions (Contreras et al., 1998a; García Camacho et al., 1999; Matthijs et al., 1996; Sáchez Mirón et al., 1999; Silva et al., 1987; Suzuki et al., 1995), earlier work with these reactors focused on nonphototrophic applications. Unlike in conventional bioreactors, light is an essential nutrient for phototrophic culture and the need for sufficient illumination significantly affects the design of an outdoor culture facility (Tredici, 1999; Sánchez Mirón et al., 1999). For most commercial processing, outdoor illumination (sunlight) appears to be the only viable option.

At present bubble columns and airlift reactors are not used as photobioreactors, except for investigational purposes; however, because of the significant potential advantages of these systems (Sánchez Mirón et al., 1999) relative to conventional tubular loop solar harvesters (Tredici, 1999), there is a need to further develop the airlift and bubble-column devices as photobioreactors. Such systems have already shown promising performance in outdoor culture of microalgae. Data suggest that a single vertical tubular photobioreactor (bubble-column or airlift design) cannot exceed about 0.2 m in diameter or light availability will be reduced severely

Correspondence concerning this article should be addressed to Y. Chisti.

(Sánchez Mirón et al., 1999). In addition, the height of a single device is limited to about 4 m for structural reasons and to reduce mutual shading of reactors in a multicolumn facility that would be necessary for any commercial-scale operation (Sánchez Mirón et al., 1999).

Further restrictions on acceptable aeration rate are posed by considerations of shear sensitivity (Chisti, 1999b; Contreras et al., 1998a; Silva et al., 1987) and light penetration (Sánchez Mirón et al., 1999). A certain minimal aeration rate is essential so that the cells do not stagnate for long in the dimly lit interior of the reactor (Sánchez Mirón et al., 1999). At the same time, there is an upper limit on the acceptable level of turbulence, because hydrodynamic forces affect certain algal cells, as reviewed recently (Chisti, 1999b). Also, in seawater, excessively high aeration rates generate persistent microbubbles that accumulate over time, thus reducing light penetration over time even at a fixed aeration rate (Sánchez Mirón et al., 1999). In addition to mixing the culture, aeration aids in removing the photosynthetically produced oxygen from the broth. Accumulation of oxygen inhibits photosynthesis. Similarly, good gas–liquid mass transfer is necessary for efficient transfer of carbon dioxide that is the carbon source in photosynthetic cultures.

This article evaluates and compares airlift and bubble-column devices, mainly in terms of hydrodynamics and transport phenomena, in anticipation of a more extensive use of these systems in producing microalgae. The focus is on fractional gas holdup, liquid circulation velocity, and the overall gas–liquid oxygen mass-transfer coefficient and the interrelationships among these variables in regimes relevant to algal culture. Data are also reported on a culture of the microalga *Phaeodactylum tricornutum*, which is a potential source of certain omega-3 polyunsaturated fatty acids of therapeutic significance.

Theoretical Developments

This section details the development of a novel theoretical equation that links the overall volumetric gas–liquid mass-transfer coefficient $k_L a_L$ with gas holdup and the superficial aeration velocity, or the principal operational variable in airlift and bubble-column reactors. The experimental data are discussed later in terms of the theoretically derived equation.

In a batch bubble column, the specific gas–liquid interfacial area a_L, the overall gas holdup ϵ, and the mean bubble diameter d_B are related (Calderbank, 1958; Chisti, 1989) by the equation:

$$a_L = \frac{6\epsilon}{d_B(1-\epsilon)}. \tag{1}$$

Equation 1 is based on fundamental principles, as discussed in depth elsewhere (Chisti, 1989). Multiplying both sides of Eq. 1 by the mass-transfer coefficient k_L produces the equation

$$k_L a_L = \frac{6k_L\epsilon}{d_B(1-\epsilon)}. \tag{2}$$

Substantial experimental evidence affirms that

$$\frac{k_L}{d_B} = \text{constant} = z, \tag{3}$$

irrespective of the flow regime and the type of fluid (Chisti and Moo-Young, 1987; Chisti, 1989, 1998). In addition, based on theory, the gas holdup is necessarily related (Chisti, 1989) with the superficial gas velocity U_G and the mean bubble rise velocity U_b, as follows:

$$\epsilon = \frac{U_G}{U_b}. \tag{4}$$

Consequently, Eq. 2 can be expressed as

$$k_L a_L = \frac{6zU_G}{U_b\left(1-\frac{U_G}{U_b}\right)} = \frac{6zU_G}{U_b - U_G}. \tag{5}$$

Equation 5 is obtained by substitution of Eq. 3 and Eq. 4 in Eq. 2. For a given fluid and flow regime, the mean velocity of bubble rise depends (Clift et al., 1978) only on the diameter of the bubble,

$$U_b = f(d_B). \tag{6}$$

For otherwise fixed conditions, the bubble size is controlled by the specific energy input E in a reactor (Chisti, 1989) and, for a bubble column, we have

$$d_B \propto E^k \propto (gU_G)^k. \tag{7}$$

The exponent k is usually around -0.4 (Bhavaraju et al., 1978; Calderbank, 1958). Thus, Eq. 5 can be written as follows:

$$k_L a_L = \frac{6zU_G}{cU_G^k - U_G}, \tag{8}$$

or

$$k_L a_L = \frac{6z}{cU_G^y - 1}. \tag{9}$$

The parameter c is close to unity in the bubble flow regime; thus,

$$k_L a_L = \frac{\Phi}{U_G^y - 1}, \tag{10}$$

where $\Phi = 6z$. Equation 10 is dimensionally consistent when the product cU_G^y is taken to be dimensionless; that is, c has the units $m^{-y}s^y$. The parameters c and y may take other values, depending on the fluid and the flow regime.

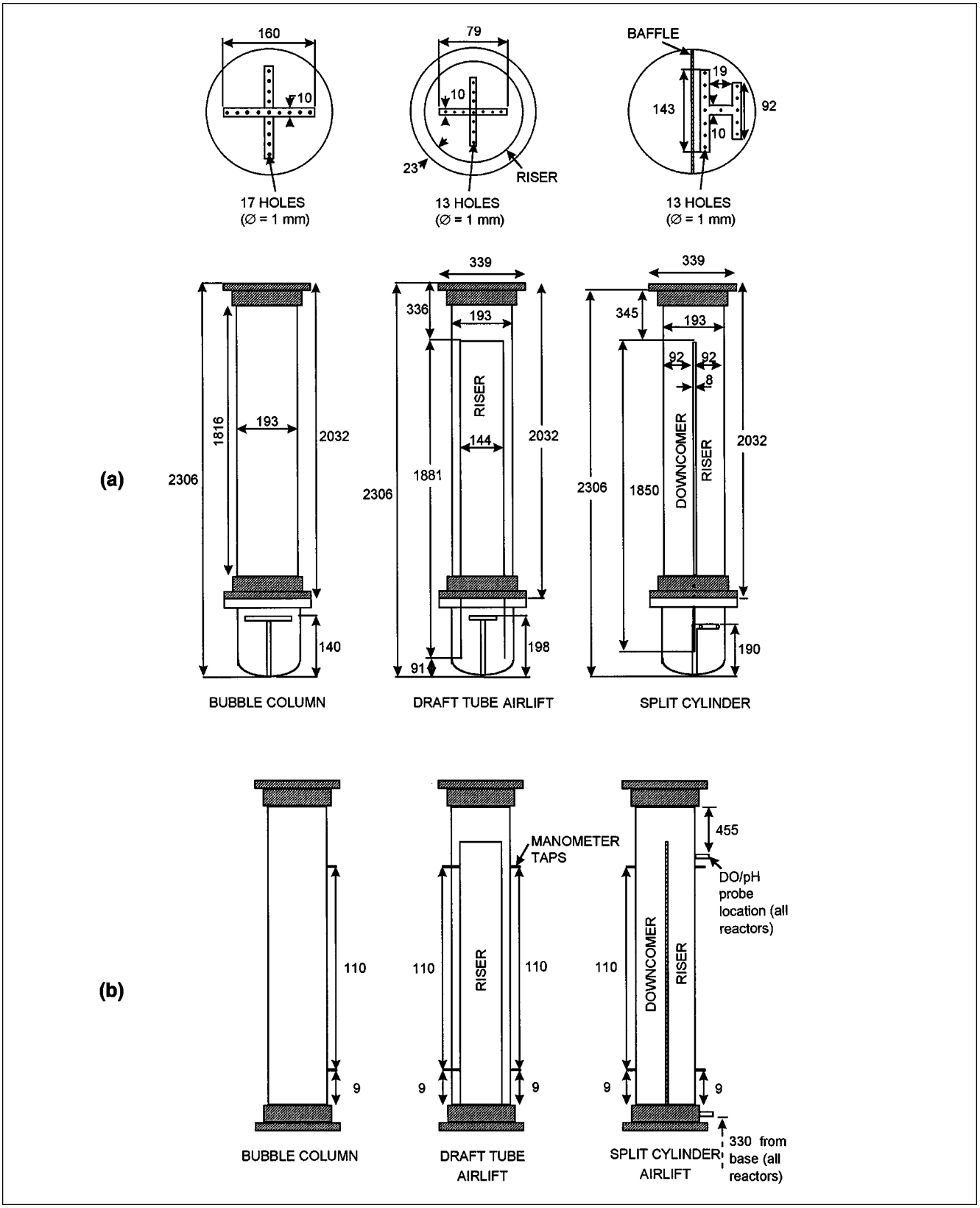

Figure 1. Reactors: (a) vessel dimensions and air sparger details; (b) location of dissolved oxygen (DO) and pH electrodes.

All dimensions in mm.

Equation 10 is derived for bubble columns, but a similar relationship can be shown to hold for airlift bioreactors. Thus, the overall volumetric gas–liquid mass-transfer coefficient $k_L a_L$ in an airlift device consists of contributions of the riser and the downcomer zones (Chisti, 1989, 1998), as follows:

$$k_L a_L = \frac{A_r (k_L a_L)_r + A_d (k_L a_L)_d}{A_r + A_d} \tag{11}$$

where A_r and A_d are the cross-sectional areas of the riser and the downcomer zones, respectively. The subscripts r and d denote the riser and the downcomer zones. Even when $\epsilon_d \neq 0$, $(k_L a_L)_d \ll (k_L a_L)_r$ (Chisti, 1989, 1998) and, generally, $A_d \leq A_r$. Consequently, in an airlift device,

$$k_L a_L \approx \frac{A_r (k_L a_L)_r}{A_r + A_d}. \tag{12}$$

Now, following the logic of Eqs. 2–9, we obtain

$$k_L a_L = \frac{\Phi_a}{U_G^y - 1}, \tag{13}$$

where $\Phi_a = 6zA_r/(A_r + A_d)$. Note that in an airlift reactor, U_b is the bubble rise velocity relative to the liquid and not relative to wall of reactor. Equations 10 and 13 are used to interpret the $k_L a_L$ data obtained in this work.

Materials and Methods

Reactors and fluids

Measurements were made in a bubble column, a split-cylinder airlift device, and a concentric draft-tube airlift vessel sparged in the draft tube. All vessels were made of 3.3-mm-thick transparent poly(methyl methyacrylate), except for the lower 0.25-m sections, which were made of stainless steel (Figure 1). The vessels were 0.193 m in internal diameter. The riser-to-downcomer cross-sectional area ratio was unity for the split cylinder and 1.24 for the draft-tube airlift vessel. The internal diameter of the draft tube was 0.144 m. The draft tube and the baffle were located 0.091 and 0.096 m from the bottoms of the reactors, respectively. The gas-free liquid height was about 2 m in all cases. Other geometric details, including those of the air spargers for the various reactors, are noted in Figure 1. Tap water and Mediterranean seawater were the liquids used. The seawater contained about 36.6 $kg \cdot m^{-3}$ total dissolved solids, almost all as inorganic salts. The ionic strength of seawater, estimated using the Langelier equation (Snoeyink and Jenkins, 1980), was 0.92.

In all cases, the specific power input in the reactors was calculated (Chisti, 1989; Chisti and Moo-Young, 1987, 1989) using the equation:

$$\frac{P_G}{V_L} = \rho_L g U_G, \tag{14}$$

where P_G is the power input due to aeration, V_L is the culture volume, g is the gravitational acceleration, and U_G is the superficial gas velocity based on the entire cross-sectional area of the reactor tube. The specific energy input per unit mass was obtained with the equation:

$$E = \frac{P_G}{\rho_L V_L} = g U_G. \tag{15}$$

All measurements were at 22 ± 2°C.

Gas holdup

The overall gas holdup in airlift reactors was measured by the volume expansion method. Inverted manometers were used to measure the separate holdup values for the riser and the downcomer zones. The overall holdup in the bubble column was measured manometrically. Both the volume expansion and the manometric methods have been described in detail and used widely (Chisti, 1989). The holdup was calculated using the equation:

$$\epsilon = \frac{\Delta h_m}{h_t} \tag{16}$$

where h_t is the vertical distance between the manometer taps, and Δh_m is the manometer reading. The location of the manometer taps is shown in Figure 1 for the various reactors.

Liquid circulation velocity

A small amount of concentrated sulfuric acid was added to the reactor to reduce the pH to around 4, and the reactor was bubbled with air ($U_G \sim 0.02$ $m \cdot s^{-1}$) for at least 30 min prior to measurements. This removed most of the buffering due to dissolved carbonates and bicarbonates. The pH was raised to around pH 5 by adding sodium hydroxide (12 M). A measured amount of concentrated acid tracer was now added to the reactor instantaneously. Additions were made on the surface of the dispersion at the center of the vessel cross section. The tracer signal was followed by two identical pH electrodes positioned in the downcomer, as shown in Figure 1. The placement of electrodes attempted to minimize entrance effects, but maintained a sufficient vertical distance between the probes so that measurement inaccuracies were minimized. The signal from the pH electrodes was expressed as a normalized concentration of the H^+ ion and plotted against time (Figure 2). The dimensionless normalized concentration was defined as

$$[H^+]_{\text{Normalized}} = \frac{[H^+] - [H^+]_o}{[H^+]_\infty - [H^+]_o}, \tag{17}$$

where $[H^+]$ is the instantaneous molar concentration and subscripts o and ∞ denote initial and final equilibrium values, respectively.

The tracer response signal displayed the dampened oscillatory pattern that is characteristic of airlift reactors (Chisti and Moo-Young, 1987; Chisti, 1989). The mean linear flow velocity in the riser–downcomer loop was calculated from the time interval between adjacent tracer peaks (Figure 2) of a given

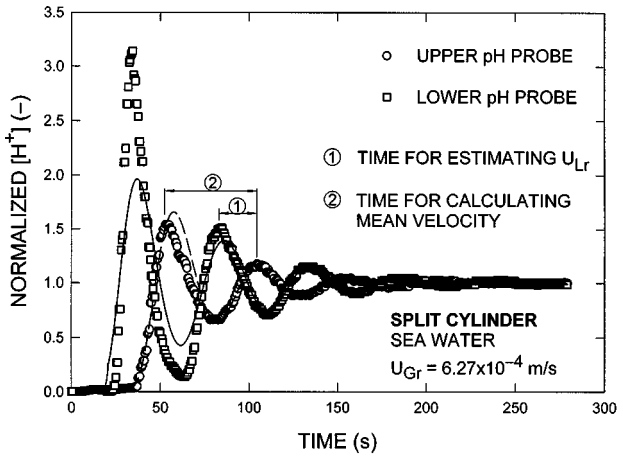

Figure 2. Normalized tracer concentration profiles from the upper and lower pH electrodes.

Time intervals used in estimating the mean loop velocity and the linear velocity in the downcomer are shown.

pH electrode and the geometry-determined length of the circulation path. The linear liquid velocity V_{Ld} in the downcomer was calculated from the time interval between the corresponding peaks (such as the second peak) of the two electrodes (Figure 2) and the known vertical distance between them.

The measured linear velocity V_{Ld} in the downcomer was related (Chisti, 1989) to the superficial velocity in the riser by the continuity relationship:

$$U_{Lr} A_r = V_{Lr} A_r(1-\epsilon_r) = V_{Ld} A_d(1-\epsilon_d), \qquad (18)$$

where V_{Lr} is the linear liquid velocity in the riser. In the split-cylinder reactor, because the cross-sectional areas of the riser and downcomer zones were identical, that is, $A_r = A_d$, Eq. 18 simplified to

$$U_{Lr} = V_{Lr}(1-\epsilon_r) = V_{Ld}(1-\epsilon_d). \qquad (19)$$

Because the superficial liquid velocity U_{Ld} in the downcomer is $V_{Ld}(1-\epsilon_d)$, U_{Lr} and U_{Ld} values were identical, irrespective of the gas holdup; thus, the mean superficial velocity of the riser–downcomer loop was the same as U_{Lr}. For the draft-tube reactor, the equivalent of Eq. 19 was

$$U_{Lr} = V_{Lr}(1-\epsilon_r) = V_{Ld}\frac{A_d}{A_r}(1-\epsilon_d). \qquad (20)$$

For both airlift reactors, the mean linear velocity V_{Loop} through the riser–downcomer loop was related to the superficial liquid velocity in the riser, as follows:

$$V_{\text{Loop}} = \frac{V_{Lr}+V_{Ld}}{2} = \frac{1}{2}\left(\frac{U_{Lr}}{(1-\epsilon_r)} + \frac{U_{Ld}}{(1-\epsilon_d)}\right). \qquad (21)$$

For the split-cylinder vessel, because U_{Lr} and U_{Ld} were identical, Eq. 21 simplified to

$$V_{\text{Loop}} = \frac{V_{Lr}+V_{Ld}}{2} = \frac{U_{Lr}}{2}\left(\frac{1}{(1-\epsilon_r)} + \frac{1}{(1-\epsilon_d)}\right). \qquad (22)$$

Gas–liquid mass-transfer coefficient

The well-known dynamic gassing-in and gassing-out methods (Chisti, 1989, 1999a) were used to measure the $k_L a_L$. Two independent measurements were made simultaneously using two dissolved oxygen (DO) electrodes, located as noted in Figure 1. Both probes provided identical $k_L a_L$ values, hence confirming the assumed well-mixed liquid phase. Measurements were made during absorption and desorption of oxygen. For absorption, the fluid was deaerated by bubbling with nitrogen until the DO concentration had declined to below 5% of air saturation. The nitrogen flow was then stopped and the bubbles were allowed to leave the liquid. A preset flow of air was now established, and the increase in DO concentration was followed with time until the concentration reached almost 100% of the air saturation value. The $k_L a_L$ was calculated as the slope of the linear equation:

$$\ln\left(\frac{C^* - C_o}{C^* - C}\right) = k_L a_L (t - t_o), \qquad (23)$$

where C^* is the saturation concentration of DO, C_o is the initial concentration of DO at time t_o when a hydrodynamic steady state has been reestablished upon commencement of aeration, and C is the DO concentration at any time t (Chisti, 1989, 1999a). Both the absorption and desorption methods gave identical values of $k_L a_L$ under identical hydrodynamic conditions. Only the $k_L a_L$ values measured during oxygen absorption are reported here.

Algal culture

Phaeodactylum tricornutum UTEX 640 was the microalga used. The culture was obtained from the collection of the University of Texas, Austin. The inoculum for the photobioreactors was grown indoors under artificial light (230 $\mu\text{E}\cdot\text{m}^{-2}\text{s}^{-1}$ light flux at the vessels' surface) in a 20-L bubble column. The medium was prepared in seawater as previously detailed (Sánchez Mirón et al., 1999).

Outdoor cultures were carried out "batchwise," simultaneously in all reactors, during August 5–16, 1999. The mean outdoor irradiance during this period was 200 ± 69 $\mu\text{E}\cdot\text{m}^{-2}\cdot\text{s}^{-1}$ at 8:00 h, rising to a mean daily value of $1{,}056 \pm 278$ $\mu\text{E}\cdot\text{m}^{-2}\cdot\text{s}^{-1}$ at noon. The reactors were located in Almería (36° 50′ N, 2° 27′ W), Spain. The biomass concentration at inoculation was about 0.07 $\text{g}\cdot\text{L}^{-1}$. The aeration rate during culture was constant at a U_G value of 0.011 $\text{m}\cdot\text{s}^{-1}$, corresponding to a specific power input of 109 $\text{W}\cdot\text{m}^{-3}$. The temperature was controlled at 20°C by circulating chilled water through a jacket that surrounded the lower steel portion of the reactors. Seawater was added from time to time to make up the losses. Other aspects of the culture methodology have been detailed previously (Sánchez Mirón et al., 1999).

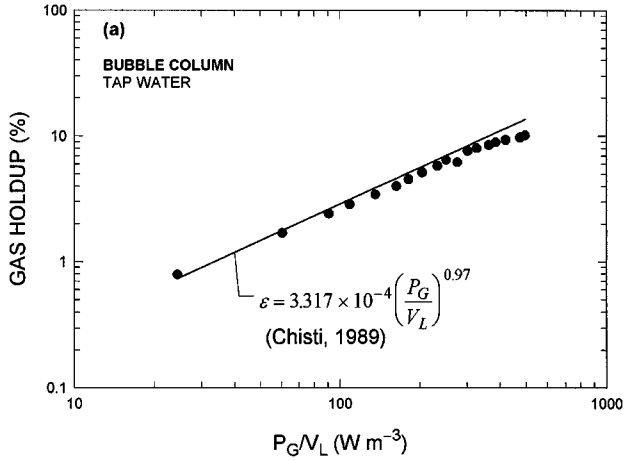

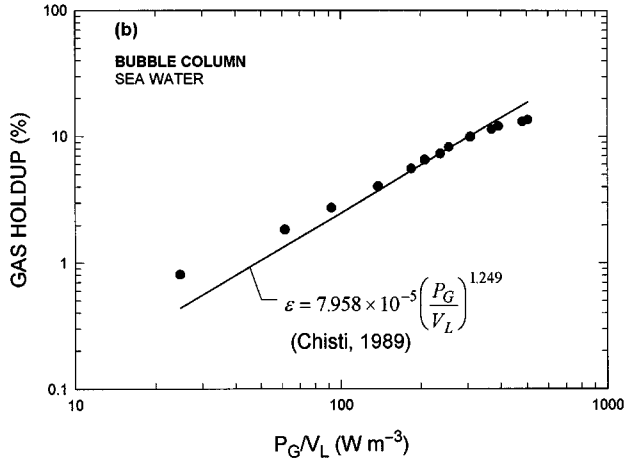

Figure 3. Comparison of the measured gas holdup in the bubble column with the correlations of Chisti (1989): (a) tap water; (b) sea- or saltwater.

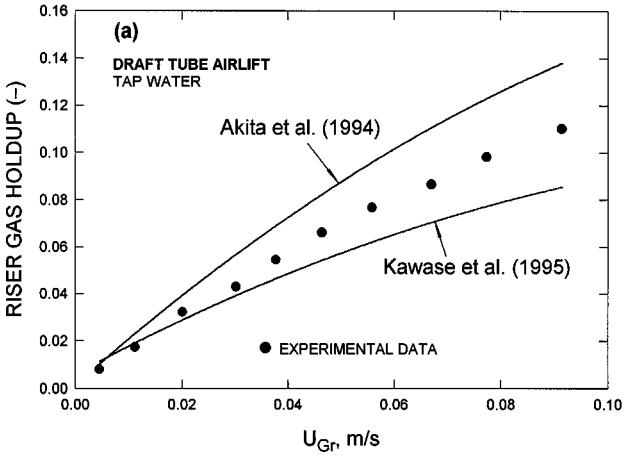

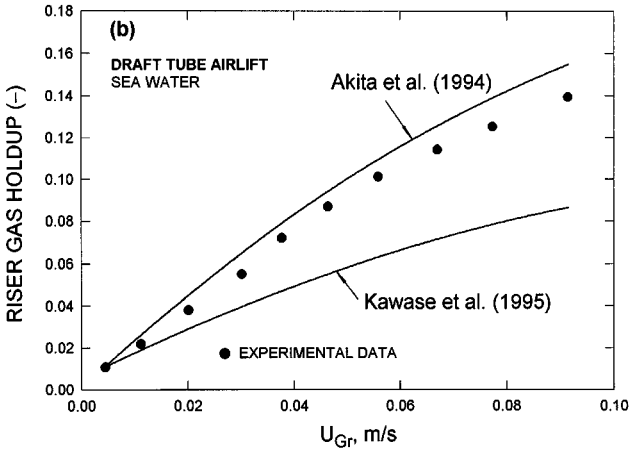

Figure 4. Comparison of the measured riser gas holdup in the draft-tube airlift vessel with published data: (a) tap water; (b) sea- or saltwater.

Results and Discussion

Gas holdup

Numerous gas holdup correlations are available for bubble columns (Akita and Yoshida, 1973; Chisti, 1989; Deckwer, 1992) and airlift bioreactors (Akita et al., 1994; Chisti, 1989, 1998, 1999a; Kawase et al., 1995; Miyahara et al., 1986). While there tends to be a general agreement among the different correlations for bubble columns, this consistency is lacking for airlift reactors (Chisti, 1989, 1998). In the latter, the holdup is influenced by the induced liquid circulation rate that depends on the geometry of the flow path, the gas–liquid separating ability of the head zone of the reactor (Chisti and Moo-Young, 1993), and also the height of the airlift column (Chisti, 1989, 1998). As shown in Figure 3, the gas holdup data in the bubble column agreed closely with equations published for tap water and salt solutions (Chisti, 1989), thus confirming the accuracy of the measurements. In Figure 3, the slight deviation of the data from the correlations for specific power input values greater than about 400 W·m^{-3} is because of the change in flow regime from bubble flow to churn turbulent regime. As expected for media containing a large amount of dissolved salts, the flow transition occurs at slightly greater power input (Chisti, 1989) in seawater compared to tap water (Figure 3). Dissolved ions inhibit bubble coalescence (Akita and Yoshida, 1973; Chisti, 1989: Deckwer, 1992; Hikita et al., 1981), hence postponing flow transition to higher values of gas holdup. As shown in Figure 3, the correlation developed for 0.15 M sodium chloride solution (Chisti, 1989) is quite satisfactory for seawater, because the effect of dissolved ions on gas holdup is marginal once the ionic strength is 0.2 or greater.

In the two airlift reactors, the gas holdup values agreed less well with published data. Thus, as shown in Figures 4 and 5, the riser holdup in tap water was consistently low in comparison with the equation:

$$\frac{\epsilon_r}{(1-\epsilon_r)^4} = \frac{\lambda}{\sqrt{gd_r}} \left(\frac{gd_r^2\rho_L}{\sigma}\right)^{1/8} \left(\frac{gd_r^3\rho_L^2}{\mu_L^2}\right)^{1/12} \left(U_{Gr} - \frac{U_{Lr}\epsilon_r}{1-\epsilon_r}\right), \tag{24}$$

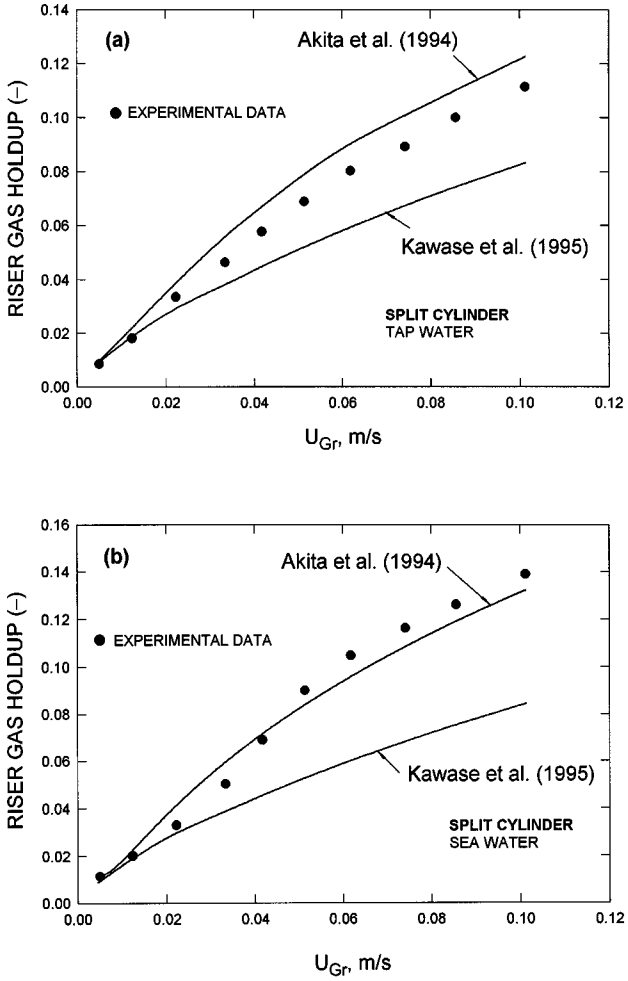

Figure 5. Comparison of the measured riser gas holdup in the split-cylinder airlift vessel with published data: (a) tap water; (b) sea- or saltwater.

established by Akita et al. (1994). In Eq. 24, the parameter λ is 0.20 for nonelectrolytes and 0.25 for electrolytes (Akita and Yoshida, 1973). The riser diameter d_r in Eq. 24 has no impact on the value of gas holdup. For both airlift devices, agreement with Eq. 24 improved greatly in seawater (Figures 4 and 5). In addition, the riser holdup in tap water did not correlate well with the equation:

$$\frac{\epsilon_r}{1-\epsilon_r} = \frac{(U_{Gr}/n)^{(n+2)/(2(n+1))}}{2^{(3n+5)/(n+1)}\left(\frac{g^n K}{\rho_L}\right)^{1/(2(n+1))}\left(1+\frac{A_d}{A_r}\right)^{3(n+2)/(4(n+1))}}, \tag{25}$$

where, for Newtonian fluids, the flow index n is unity and the consistency index K is replaced by viscosity. Equation 25 was developed by Kawase et al. (1995) using theoretical principles and assuming isotropic turbulence. Limited usefulness of Eq. 25 is apparently due to its disregard for effects of liquid circulation on gas holdup. Also, Eq. 25 does not consider effects of surface tension and dissolved ions. Moreover, the ''theoretical'' foundation of the equation is questionable because the assumption of isotropic turbulence in bubble columns and airlift reactors is not valid, even at high-energy inputs in waterlike media (Chisti, 1998; Lübbert and Larson, 1990; Lübbert et al., 1990; Okada et al., 1993). Although Eq. 25 is intended also for viscous non-Newtonian media, the assumption of isotropic turbulence in such systems is even less realistic.

Another equation for riser gas holdup in internal-loop airlift reactors is that of Miyahara et al. (1986):

$$\epsilon_r = \frac{0.4\sqrt{Fr}}{1+0.4\sqrt{Fr}\left(1+\frac{U_{Lr}}{U_{Gr}}\right)}, \tag{26}$$

where the Froude number Fr is based on the diameter of the sparger hole, that is,

$$Fr = \frac{U_{Gr}^2}{gd_o}. \tag{27}$$

Equation 26 was developed for a variety of Newtonian fluids, but not for media containing large quantities of dissolved salts. However, as shown in Figure 6 for tap water only, Eq. 26 consistently and substantially overpredicts holdup values. The comparisons in Figures 3–6 clearly demonstrate that the gas holdup data in different airlift devices are not well correlated with equations developed without considering the underlying mechanics. Numerous correlations for gas holdup in airlift devices have taken the general form $\epsilon = pU_G^q$ (Chisti and Moo-Young, 1987; Chisti, 1989, 1998; Merchuk and Gluz, 1999), but these equations are suited only to specific combinations of fluid properties and reactor geometry, because the parameters p and q are sensitive to these factors.

A superior approach to correlating gas holdup in airlift reactors is the use of the drift-flux model-type equations in combination with a mechanistic relationship for liquid circulation velocity in two-phase flow (Chisti, 1989, 1998). The drift-flux relationship for gas–liquid flow in vertical conduits takes the form:

$$\epsilon_r = \frac{U_{Gr}}{\alpha(U_{Lr}+U_{Gr})+\beta}, \tag{28}$$

where the parameters α and β have physical meanings (Chisti, 1989, 1998). As shown in Figure 7 for two representative cases including both airlift reactors and the two fluids, the riser gas holdup correlates well with Eq. 28. For the two fluids (Figure 7), a mean β value of 0.30 $\mathrm{m \cdot s^{-1}}$ was in the expected range for bubble rise velocities. The parameter α differed for the two reactors (Figure 7) because the shapes of the flow channels were quite different for the two cases. The riser of the draft-tube airlift had a circular cross section, whereas in the split-cylinder device the riser cross section was a semicircle. In view of the fit in Figure 7, the induced liquid circulation rate clearly needs to be taken into account for

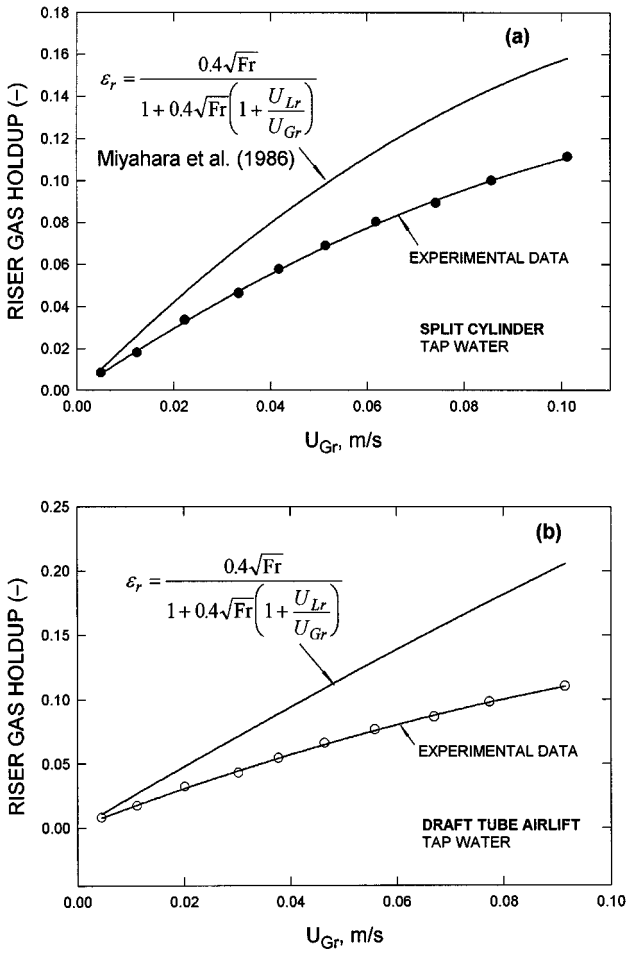

Figure 6. Comparison of the measured riser gas holdup in the two airlift vessels with Eq. 26 of Miyahara et al.

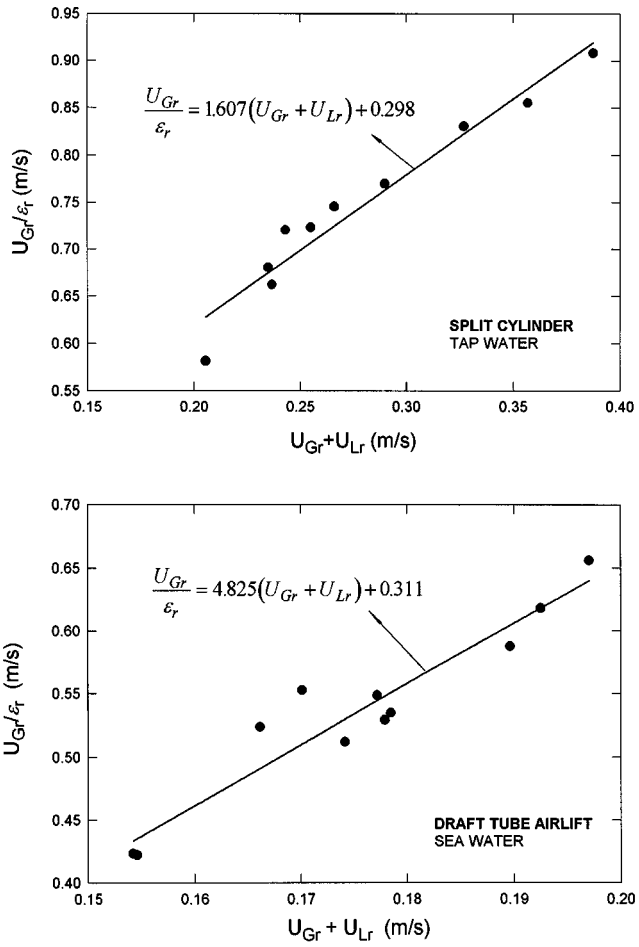

Figure 7. Plots of Eq. 28 for two representative cases in the airlift vessels.

predicting gas holdup. In circular channels an α-value of unity implies a flat radial velocity profile. In view of the high α-value (Figure 7) in the split-cylinder device, the radial velocity profile was apparently parabolic in the semicircular channel.

Unfortunately, in an airlift device, the induced liquid circulation velocity is not usually known *a priori*, and therefore for predictive purposes, the theoretical Eq. 28 needs to be used in combination with other equations (Chisti, 1989, 1998). The need to predict gas holdup arises mainly because of the need to know the gas–liquid mass-transfer coefficient that depends on holdup. As shown in the following subsection on the effect of liquid circulation velocity on mass transfer, Eq. 28 in combination with a well-known mechanistic model for the induced liquid circulation velocity (Chisti, 1989), provided a reliable method for predicting the overall volumetric mass-transfer coefficient ($k_L a_L$) values in airlift reactors.

With few exceptions (Ganzeveld et al., 1995; Wenge et al., 1996), the relationship between the riser and the downcomer gas holdups has been generally expressed (Contreras et al., 1998b) in the form:

$$\epsilon_d = a\epsilon_r, \tag{29}$$

where the parameter a is a constant (Chisti, 1989). However, as was recently pointed out (Contreras et al., 1998b), Eq. 29 disregards the fact that gas holdup in the downcomer remains zero until a finite holdup value has been established in the riser (Wenge et al., 1996). Consequently, a better correlation between riser and downcomer gas holdups has been proposed (Contreras et al., 1998b) in the form:

$$\epsilon_d = a\epsilon_r - b. \tag{30}$$

The meanings of parameters a and b in Eq. 30 have been discussed elsewhere (Contreras et al., 1998b). Representative data in tap water and seawater are shown in Figure 8 plotted according to Eqs. 29 and 30. Clearly, Eq. 30 provides a superior fit of the data, all of which displays a distinct nonzero x-intercept. Similar behavior was seen for the draft-tube airlift device.

In the two airlift reactors, the overall holdup ϵ was measured by height displacement, where the holdup values in the riser (ϵ_r) and downcomer (ϵ_d) were determined manometrically. In addition to the direct measurements, a value of the overall holdup also could be calculated using the measured

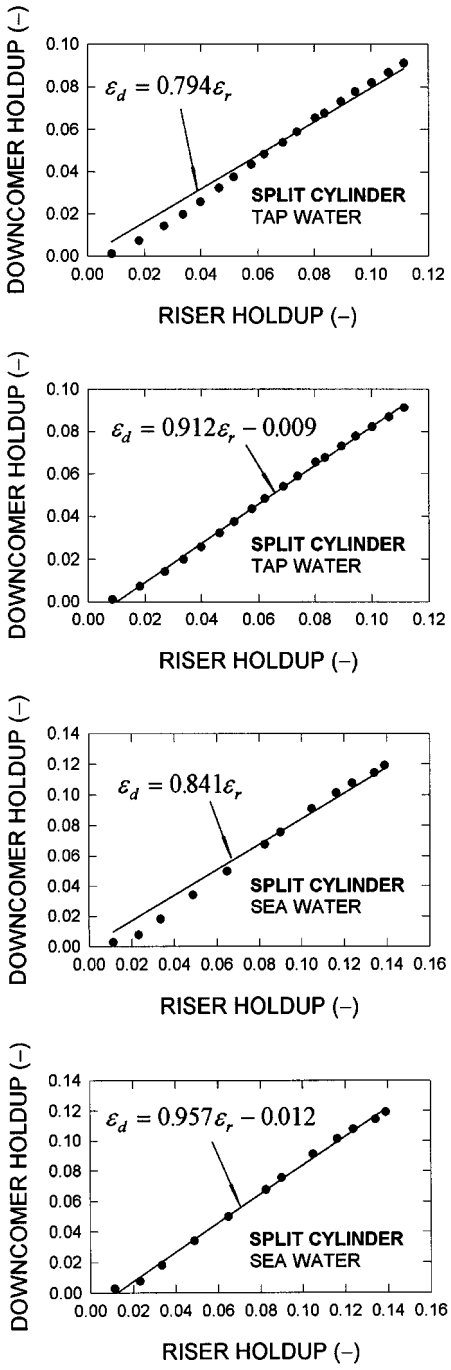

Figure 8. Relationship between riser and downcomer gas holdups.

Split-cylinder data are shown for tap water and seawater plotted according to Eq. 29 and Eq. 30.

riser and downcomer gas holdups (Chisti, 1989), as follows:

$$\epsilon = \frac{A_r \epsilon_r + A_d \epsilon_d}{A_r + A_d}. \tag{31}$$

Equation 31 is based on geometric reasoning and it is an exact relationship for the kinds of airlift reactors used here

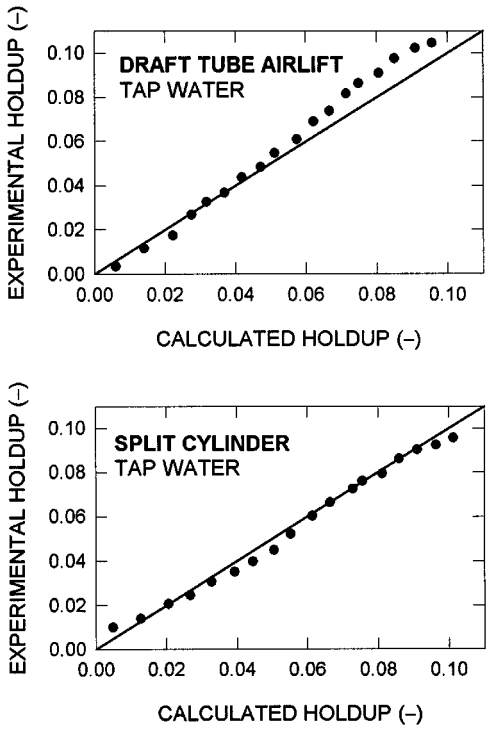

Figure 9. Comparison of the measured overall holdup with values calculated according to Eq. 31 for two cases in airlift reactors; diagonals represent an exact agreement.

(Chisti, 1989). As shown in Figure 9 for two representative cases, excellent agreement is observed between the measured overall holdup and the values calculated with Eq. 31. This confirms internal consistency of manometrically measured gas holdup values in the riser and downcomer while also validating Eq. 31.

The various gas holdup values in the three reactors used are compared in Figure 10 for the two fluids. Generally, for a given specific power input, the riser gas holdup in the two airlift vessels is comparable to the overall holdup in the bubble column; however, the downcomer gas holdup is significantly less than the holdup in the riser (Figure 10). Consequently, the overall holdup of the airlift vessels is somewhat lower than in the bubble column. In comparison with the riser holdup, the holdup in the downcomer is much lower at the lower power input values than at higher ones (Figure 10). This is because under conditions of low-power input the mean bubble size in the riser is bigger, and bigger bubbles are less readily dragged into the downcomer with the flow.

Gas–liquid mass transfer

Much more information exists on gas–liquid mass transfer in bubble columns than exists in airlift devices (Akita and Yoshida, 1973; Chisti, 1989, 1998, 1999a; Deckwer, 1992). In addition, compared to airlift reactors, fewer factors influence $k_L a_L$ values in bubble columns and, for a given fluid, the $k_L a_L$ data obtained in different columns generally compare well irrespective of the column aspect ratio (Chisti, 1989), so

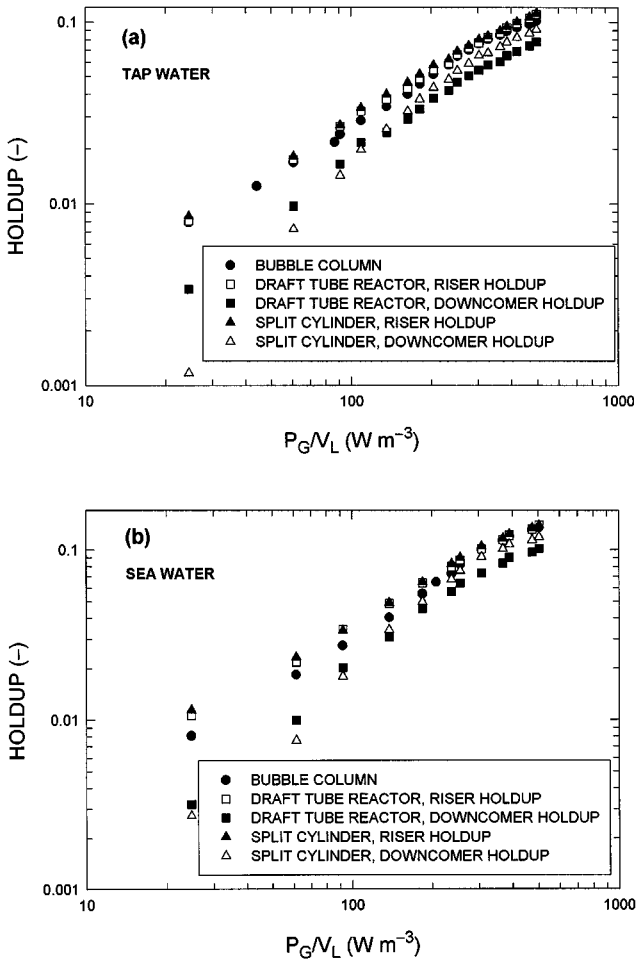

Figure 10. Comparison of various gas holdup values in the three reactors for various values of specific power input: (a) tap water; (b) seawater.

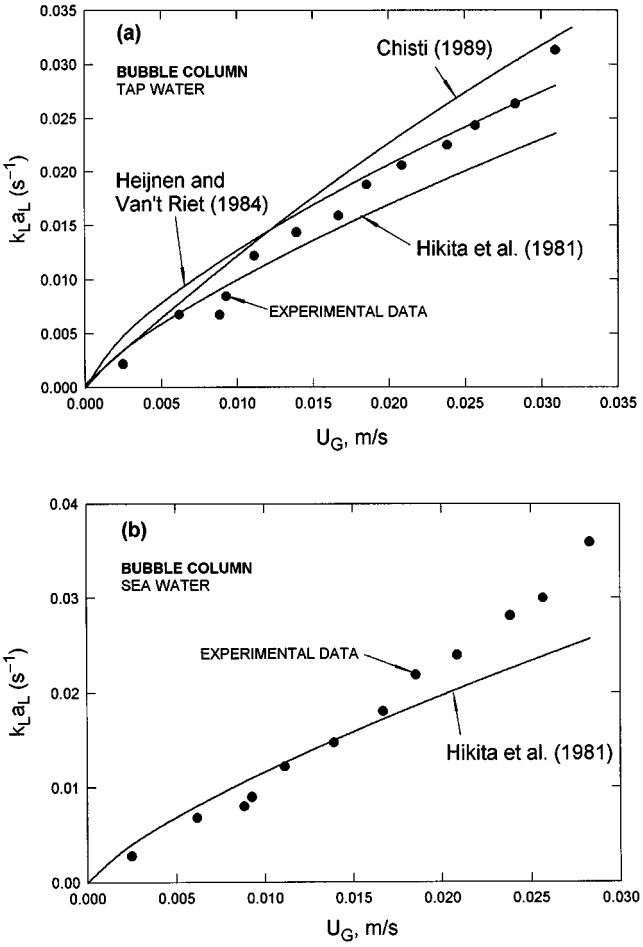

Figure 11. Comparison of the measured k_La_L in bubble column with the published correlations: (a) tap water; (b) sea- or saltwater.

long as the column diameter exceeds about 0.1 m, as was the case here. Because of this consistency, accuracy of the mass-transfer measurements may be demonstrated by comparing data obtained in a bubble column with other well-established reference data before applying the same measurement method to airlift reactors, or before new data are interpreted in a novel way. As shown in Figure 11 for the bubble column, the measured k_La_L data agreed remarkably well with some of the well-known correlations in both fluids. The correlations used in the comparison were as follows.

1. That of Hikita et al. (1981):

$$k_La_L = \frac{14.9g\phi}{U_G}\left(\frac{U_G\mu_L}{\sigma}\right)^{1.76}\left(\frac{\mu_L^4 g}{\rho_L\sigma^3}\right)^{-0.248}\left(\frac{\mu_G}{\mu_L}\right)^{0.243} \times\left(\frac{\mu_L}{\rho_L D_L}\right)^{-0.604}, \quad (32)$$

whereas ϕ was 1.0 for tap water. For seawater the ϕ-value was 1.2, as recommended by Hikita et al. (Chisti, 1999a). The other variables in Eq. 32 are gravitational acceleration g, the surface tension σ, the viscosities of the gas (μ_G) and the liquid (μ_L) phases, the density ρ_L of the liquid phase, and the diffusivity D_L of oxygen in the liquid.

2. The one recommended by Heijnen and Van't Riet (1984):

$$k_La_L = 0.32U_G^{0.7}. \quad (33)$$

3. That established by Chisti (1989):

$$k_La_L = 2.39\times10^{-4}\left(\frac{P_G}{V_L}\right)^{0.86}. \quad (34)$$

For the comparison in Figure 11, Eq. 34 was expressed in terms of the superficial gas velocity.

Having validated the k_La_L data, let us see how the theoretically developed Eq. 10 and Eq. 13 fare in correlating the measurements. As shown in Figure 12, for all six combinations of reactors and fluids, the k_La_L data correlated exceptionally well with equations of the same general form as Eq. 10. Use of Eq. 10 is preferred to purely empirical relationships of the type $k_La_L = aU_G^b$ that have been used commonly

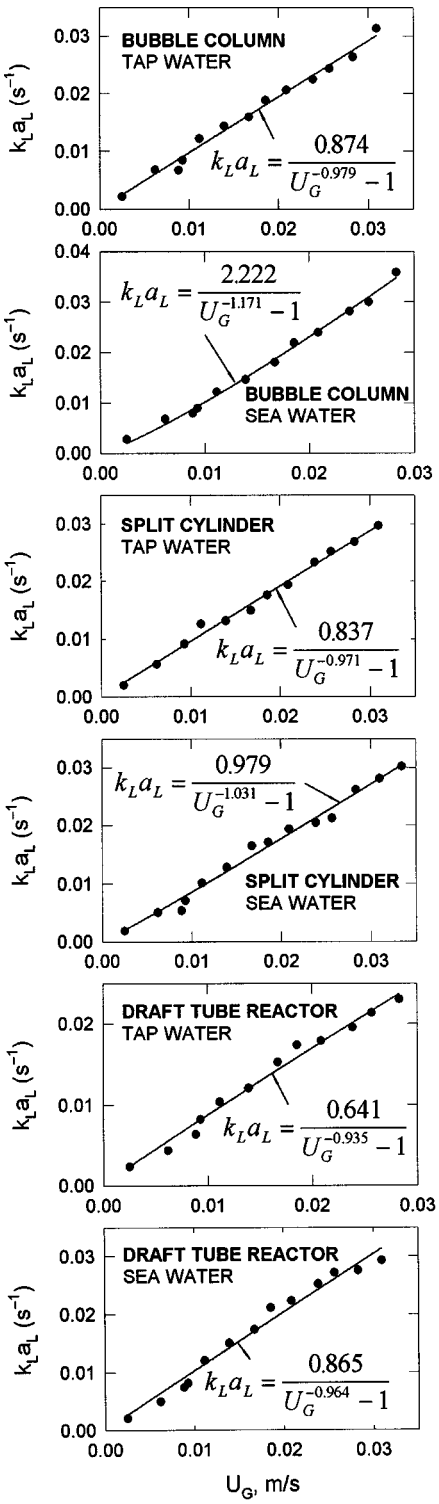

Figure 12. Correlation of the measured $k_L a_L$ with the superficial aeration velocity U_G according to Eq. 10 or Eq. 13; data are shown for all reactor-fluid combinations.

(Chisti, 1989, 1998, 1999a; Heijnen and Van't Riet, 1984; Merchuk and Gluz, 1999). This is particularly so for the airlift reactors, because there is no general agreement on the values of a and b for these reactors, even for a given fluid and reactor geometry (Chisti, 1989, 1998, 1999a).

The parameters Φ_a (or Φ) and y in Eq. 13 depend on the reactor and the fluid, as can be seen in Figure 12. For a given type of reactor, the Φ_a (or Φ) value is always greater for seawater than for tap water (Figure 12), whereas y is close to unity for all cases. Note that these values apply to bubble-flow regime, which prevailed over most of the operational range tested. A comparison of the data in Figure 12 revealed that in the bubble column, the $k_L a_L$ in seawater was always greater than in tap water by a factor of 2.5 $[(U_G^{-0.979} - 1)/(U_G^{-1.171} - 1)]$, or 1.3 at $U_G = 0.03$ m·s^{-1}, so long as the superficial gas velocity exceeded 0.01 m·s^{-1}. Similarly, in the draft-tube airlift device, the sewater $k_L a_L$ was always 15–20% greater than in tap water. However, in the split-cylinder device, $(k_L a_L)_{\text{sea water}}/(k_L a_L)_{\text{tap water}}$ was about 0.85 at a gas velocity of < 0.01 m·s^{-1}, and increased to 0.94 when the velocity approached 0.03 m·s^{-1}. For tap water, the $k_L a_L$ in the split cylinder was a marginal 2% less than in the bubble column. In contrast, the $k_L a_L$ values in the draft-tube device were typically 12–15% lower than in the bubble column. In sea water, the $k_L a_L$ values in the split-cylinder device were 15–30% reduced relative to the bubble column, whereas in the draft-tube airlift the reduction was 0–20%, depending on the gas flow rate. These changes in $k_L a_L$ values relative to those in the bubble column were largely explained by a reduced gas holdup in the airlift units.

In obtaining the theoretical Eq. 10, the k_L/d_B ratio was assumed to be constant. Although a constancy of the k_L/d_B ratio has been validated previously (Chisti and Moo-Young, 1987; Chisti, 1989), direct evidence from the present study further supported the assumption, as discussed next.

Relationship Between Gas Holdup and Mass-Transfer Coefficient. As expected from Eq. 2, plots of $k_L a_L$ against $6\epsilon_r/(1-\epsilon_r)$ were linear (Figure 13), confirming that the k_L/d_B ratio (that is, the slope) was constant for a given fluid. Thus, for seawater, a mean k_L/d_B value of 0.042 s^{-1} was within $\pm 8\%$ for the two airlift reactors, whereas the value for tap water (0.056 s^{-1}) was within $\pm 11\%$ of the mean for both reactors. In the bubble column the k_L/d_B values were 0.055 s^{-1} and 0.062 s^{-1} for seawater and tap water, respectively. Clearly, in a given fluid, the k_L/d_B ratio was little affected by the type of gas-agitated reactor used, and this was consistent with earlier observations (Chisti, 1989). The magnitude of the k_L/d_B values obtained compared well with earlier reported ones: for example, a value of 0.05 s^{-1} (Chisti, 1989) was reported in 0.15 M sodium chloride, and it was within 20% of that for seawater in the present study. The observed k_L/d_B values agreed with the equation within $\pm 10\%$:

$$\frac{k_L}{d_B} = 5.63 \times 10^{-5} \left(\frac{g D_L \rho^2 \sigma}{\mu_L^3} \right)^{0.5} e^{-0.131 C_s^2}. \qquad (35)$$

In Eq. 35 C_s is the concentration of solids in suspension (wt/vol %), D_L is the diffusivity of gas in liquid, and σ is the interfacial tension. Equation 35 was developed for air–water dispersions and for suspensions with a waterlike continuous phase (Chisti and Moo-Young, 1987; Chisti, 1989).

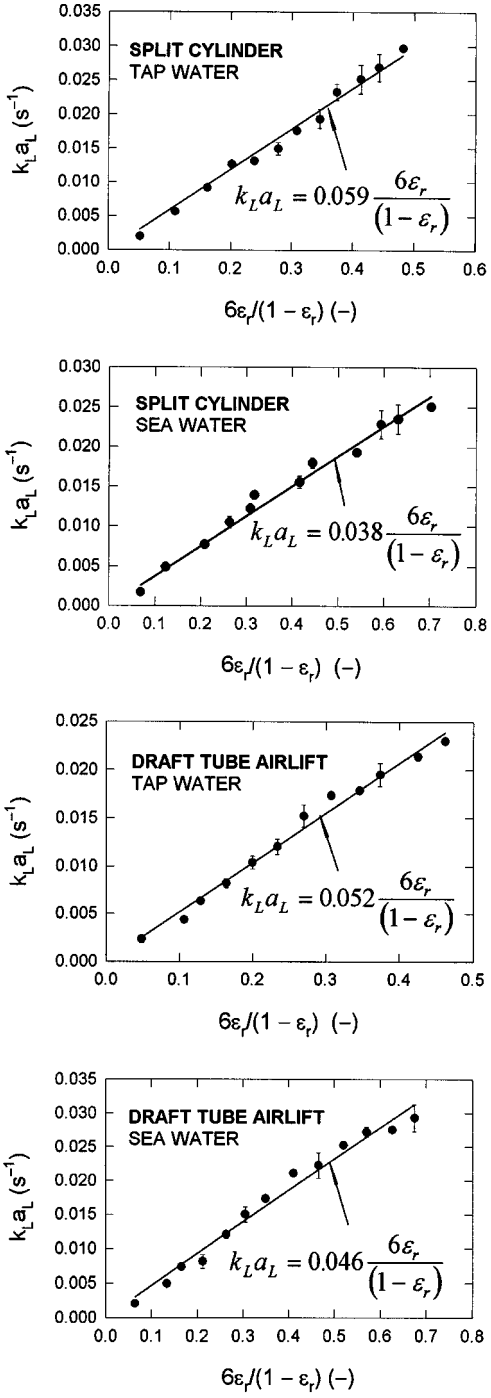

Figure 13. Correlation of the measured $k_L a_L$ and the measured riser holdup ϵ_r in airlift reactors according to Eq. 2; vertical bars denote standard deviation of selected mean $k_L a_L$ values.

The k_L/d_B ratio in seawater was significantly less than in tap water (Figure 13); thus, for a given bubble diameter the k_L value was lower in seawater. This made sense, as k_L is proportional to D_L or $\sqrt{D_L}$, depending on the situation (Chisti, 1989) and, relative to pure water, dissolved ions reduce diffusivity of oxygen. As previously noted (the section on gas–liquid mass transfer; Figure 12), the $k_L a_L$ values in seawater were always greater than in tap water. Because the presence of salts reduced k_L, an enhancement of $k_L a_L$ was explained by an increase in the specific interfacial area a_L in the presence of salts. The increase in a_L more than compensated for a decline in the k_L value.

Effect of Liquid Circulation Velocity on Mass Transfer. Measurements of liquid circulation velocity are important in themselves, but here the discussion is restricted only to the impact of liquid circulation on gas holdup and the mass-transfer coefficient values. A well-known and theoretically based model for predicting the induced liquid circulation velocity in an airlift device has been published (Chisti, 1989) as:

$$U_{Lr} = \sqrt{\frac{2g(\epsilon_r - \epsilon_d)h_D}{\frac{K_T}{(1-\epsilon_r)^2} + K_B\left(\frac{A_r}{A_d}\right)^2 \frac{1}{(1-\epsilon_d)^2}}}. \qquad (36)$$

In Eq. 36, h_D is the height of dispersion, and K_T and K_B are the frictional loss coefficients for the top and the bottom zones of the airlift loop. Equation 36 is based on principles of energy conservation, and it has been repeatedly validated for a broad range of scales and configurations of airlift devices (Abashar et al., 1998; Chisti, 1989, 1998). When K_T and K_B are approximately equal, as expected for the reactors in Figure 1, Eq. 36 simplifies to:

$$U_{Lr} = \sqrt{\frac{2g(\epsilon_r - \epsilon_d)h_D}{\left[\frac{1}{(1-\epsilon_r)^2} + \left(\frac{A_r}{A_d}\right)^2 \frac{1}{(1-\epsilon_d)^2}\right]K_B}}. \qquad (37)$$

The measured values of the riser and downcomer gas holdup were used in Eq. 37 for predicting the U_{Lr} value. The best fit K_B value, that is, one that produced the closest agreement between predicted and measured U_{Lr} values, was 4.5. As shown in Figure 14, the predicted and the measured values of U_{Lr} agreed within $\pm 15\%$ for both tap and seawater. A K_B value of 4.6 was calculated (Chisti, 1989) using the geometric parameters A_d and A_b for the reactor and the published equation:

$$K_B = 11.4\left(\frac{A_d}{A_b}\right)^{0.79}. \qquad (38)$$

The K_B determined with Eq. 38 and that determined by fitting the U_{Lr} data agreed within 3% of the best fit value of 4.5.

As shown in Figure 15 for the bubble-flow regime, the driving force for liquid circulation, that is, the difference between the riser and the downcomer gas holdup values, remained fairly constant once the specific power input had exceeded about 25 $W \cdot m^{-3}$ in the split-cylinder airlift device. Correspondingly, the liquid circulation velocity rose sharply with the gas flow rate, attaining an almost constant value that was not particularly sensitive to further increases in the aeration

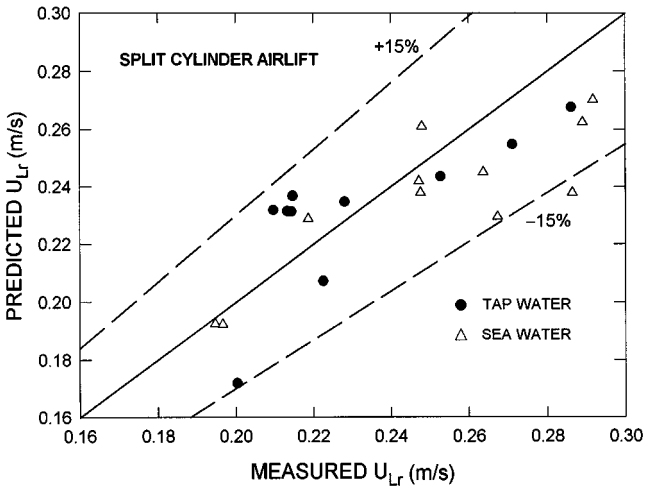

Figure 14. Predicted vs. measured superficial liquid velocities in the riser of the split-cylinder airlift reactor.

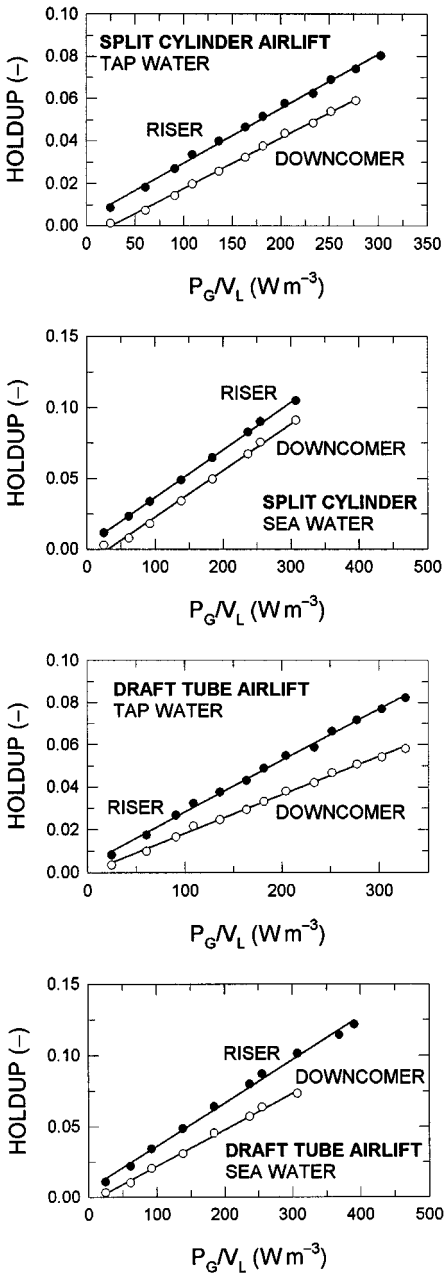

Figure 15. Variation of the riser and downcomer gas holdup values with the specific power input in the airlift reactors.

rate. Compared to the split-cylinder airlift device, in the draft-tube reactor, the $(\epsilon_r - \epsilon_d)$ value showed a slight increase as the gas flow rate increased (Figure 15), hence the plateau region of the liquid circulation velocity vs. power input curve had a slight positive slope over the entire range of aeration rates tested (Figure 15). Compared to the split-cylinder device, and despite a greater circulation driving force, the U_{Lr} value was lower in the draft-tube reactor, and this reduced the ability of the liquid to drag bubbles into the annular downcomer. The relatively lower U_{Lr} value in the draft-tube reactor was explained by a bigger A_r/A_d ratio for that reactor and the greater resistance of its circulatory channel (that is, a higher K_B relative to the split cylinder), as expected from Eq. 37.

Having validated Eq. 37, let us see how it can be used to predict the mass-transfer coefficient, $k_L a_L$. For predicting the $k_L a_L$ values, Eqs. 37 and 28 are solved simultaneously to calculate the riser holdup and the U_{Lr} value. Equation 30 is then used to calculate the downcomer gas holdup. The earlier determined k_L/d_B values (Figure 13) are then used to calculate the $k_L a_L$. Figure 16 compares the predicted and the directly measured values of $k_L a_L$, revealing a remarkably good agreement. The agreement in Figure 16 lends additional support to the various mechanistic equations used in the predicting and confirms the $k_L a_L$ prediction methodology used.

The $k_L a_L$ values in all reactors were such that accumulation of photosynthetically generated oxygen did not occur during culture, even at a relatively low aeration velocity of 0.011 m·s^{-1} ($\sim$110-W·m^{-3}-specific power input), as shown in Figure 17. The DO concentration in Figure 17 followed a cyclic pattern in all reactors because the oxygen generation rate increased from dawn to solar noon as the irradiance level peaked. Oxygen generation rate then declined through the afternoon and night. As shown in Figure 17, the DO concentration remained at $\leq$100% of air saturation, except on two occasions when the concentration rose to $\sim$110% of air saturation value in the bubble column. In contrast, in conventional tubular loop photobioreactors for algal culture, the concentration of DO commonly reaches $\geq$400% of air saturation value (Sánchez Mirón et al., 1999; Tredici, 1999). DO concentrations exceeding about 120% of air saturation are known to inhibit photosynthesis and otherwise damage the culture.

The data in Figure 17 confirm the existence of oxygen mass-transfer limitation, at the aeration rate used, for all those occasions (that is, 4 of 12 days in the bubble column) when the DO concentration exceeded 100% of the air saturation value. In airlift and bubble-column photobioreactors, low

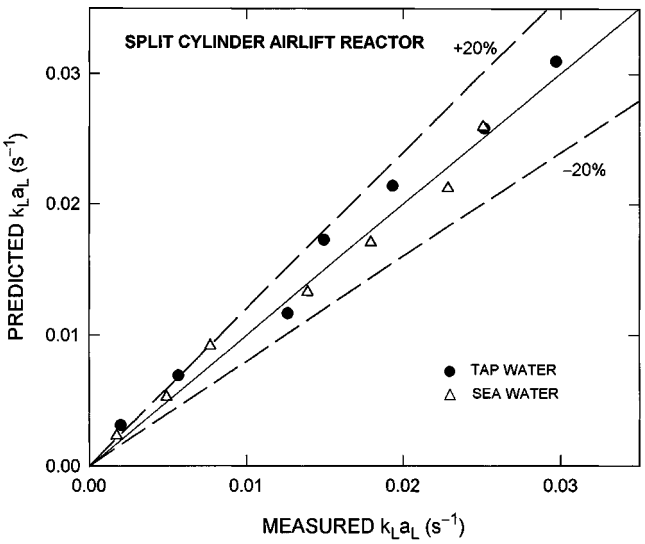

Figure 16. Predicted vs. measured k_La_L values in the split-cylinder airlift reactor.

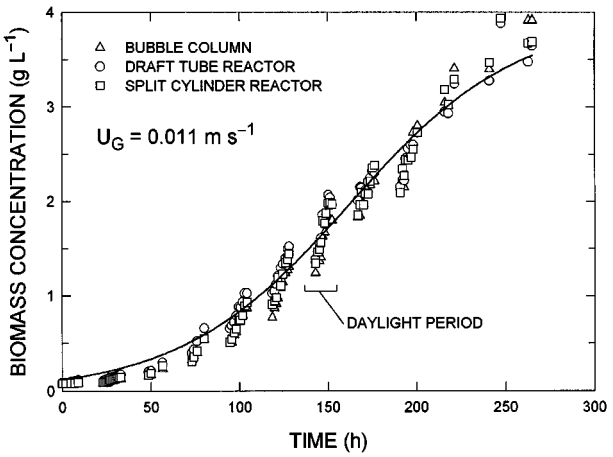

Figure 18. Outdoor batch culture profiles of *P. tricornutum* in the three bioreactors during August 5–16, 1999.

aeration rates corresponding to a power input of <120 W·m^{-3} are necessary to reduce the formation of stable microbubbles that reduce light penetration (Sánchez Mirón et al., 1999). However, low aeration rates reduce radial mixing. This effect can be countered by using larger sparger holes to increase the size of bubbles (Sánchez Mirón et al., 1999). Larger bubbles tend to improve mixing. Also, cyclic variation of aeration rate may be necessary for attaining the right balance between the conflicting demands of low gas holdup (light penetration), good mass transfer, and mixing.

Culture performance

The oxygen evolution and removal behavior during culture has already been discussed in the previous section (Figure 17). The biomass growth profiles are shown in Figure 18 for the three reactors. In batch culture, at least at the low aeration rate used (Figure 18), there was no significant difference in culture performance in the three bioreactors. This observation was consistent with the fairly similar values of gas holdup and the k_La_L measured earlier in the reactors. In all cases, the mean value of the maximum specific growth rate was 0.022 h^{-1}, which is high for *P. tricornutum*. Note that this value is a mean for the entire culture duration. Within any one daylight period, the biomass concentration increased rapidly, as shown in Figure 18; however, there was some loss of biomass during the night because a portion of the intracellular stored carbohydrate was consumed by respiration. The biomass concentration rose again during the next light period, attaining a higher value than in the previous light period. The nighttime decline could be avoided if sufficiently intense artificial illumination was provided, but this option is not practicable.

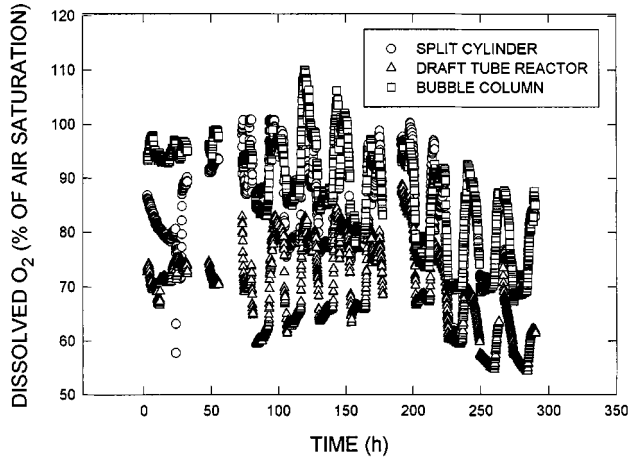

Figure 17. Changes in DO concentration during culture of *P. tricornutum* in the three bioreactors.

Concluding Remarks

In view of the findings discussed, the principal conclusions are as follows:

1. The gas holdup and k_La_L in bubble column are satisfactorily predicted with the available correlations. In contrast, existing nonmechanistic correlations perform poorly in predicting the behavior of airlift bioreactors. Hydrodynamic and oxygen-transfer characteristics of seawater are essentially equivalent to those of aqueous sodium chloride (0.15 M).

2. Equations 10 and 13, developed through an analysis of the underlying fundamentals, describe exceptionally well the relationship between k_La_L and the superficial gas velocity in all reactors. The two parameters in these equations depend on the properties of the fluid and the reactor.

3. In airlift reactors, the gas holdup, and phase velocity data are consistent with the drift-flux model equation. The relationship among the induced liquid circulation velocity, the reactor geometry, and the gas holdup difference driving force for liquid circulation is well described by the theoretically developed Eq. 37.

4. In airlift vessels, the interdependence of riser and downcomer gas holdup values is best expressed as Eq. 30, rather than the often used Eq. 29.

5. The ratio of true mass-transfer coefficient to bubble diameter, that is, k_L/d_B, is constant for a given fluid–reactor combination. Constancy of the k_L/d_B ratio, in combination with Eqs. 28, 30, and 37, allow a good prediction of the $k_L a_L$ value.

6. Culture studies confirm that sufficient oxygen is removed and a significant accumulation is prevented even when the aeration power input is around 110 $W \cdot m^{-3}$.

7. Performance of the three types of reactors was equivalent under the conditions tested. In all cases, a maximum specific growth rate of 0.022 h^{-1} was achieved in batch culture and the final *P. tricornutum* biomass concentration attained was high at $\sim 4 kg \cdot m^{-3}$.

Pneumatically agitated bubble columns and airlift devices clearly attain the requisite value of $k_L a_L$ and the induced liquid circulation velocity at a relatively low power input ($\leq 120 W \cdot m^{-3}$) for practicable culture of microalgae. So far, the data do not suggest a clear preference for one type of reactor over another of the three kinds evaluated. A more exhaustive assessment is necessary over a range of culture conditions. Further studies are underway with *P. tricornutum* in batch and continuous culture at various dilution rates, aeration conditions, and levels of outdoor illumination (seasons).

Acknowledgments

This work was supported by CICYT (BIO-98-0522), Spain, and the European Commission (Project BRPR CT97-0537).

Notation

A_b = cross-sectional area for flow under the baffle or draft tube, m^2
d_o = sparger hole diameter, m
q = exponent
t_o = initial or start time, s
U_{Gr} = superficial gas velocity in the riser zone, $m \cdot s^{-1}$
ϵ_r = fractional gas holdup in the riser
μ_G = viscosity of gas, $Pa \cdot s$
μ_L = viscosity of liquid, $Pa \cdot s$
ρ_L = density of the liquid, $kg \cdot m^{-3}$
σ = interfacial tension, $N \cdot m^{-1}$

Literature Cited

Abashar, M. E., U. Narsingh, A. E. Rouillard, and R. Judd, "Hydrodynamic Flow Regimes, Gas Holdup, and Liquid Circulation in Airlift Reactors," *Ind. Eng. Chem. Res.*, **37**, 1251 (1998).

Akita, K., and F. Yoshida, "Gas Holdup and Volumetric Mass Transfer Coefficient in Bubble Columns," *Ind. Eng. Chem. Process Des. Dev.*, **12**, 76 (1973).

Akita, K., O. Nakanishi, and K. Tsuchiya, "Turn-Around Energy Losses in an External-Loop Airlift Reactor," *Chem. Eng. Sci.*, **49**, 2521 (1994).

Bhavaraju, S. M., T. W. F. Russell, H. W. Blanch, "The Design of Gas Sparged Devices for Viscous Liquid Systems," *AIChE J.*, **24**, 454 (1978).

Calderbank, P. H., "Physical Rate Processes in Industrial Fermentations: I. The Interfacial Area in Gas-Liquid Contacting with Mechanical Agitation," *Trans. Inst. Chem. Eng.*, **36**, 443 (1958).

Chisti, Y., and M. Moo-Young, "Airlift Reactors: Characteristics, Applications and Design Considerations," *Chem. Eng. Commun.*, **60**, 195 (1987).

Chisti, Y., and M. Moo-Young, "On the Calculation of Shear Rate and Apparent Viscosity in Airlift and Bubble Column Bioreactors," *Biotechnol. Bioeng.*, **34**, 1391 (1989).

Chisti, Y., and M. Moo-Young, "Improve the Performance of Airlift Reactors," *Chem. Eng. Prog.*, **89**(6), 38 (1993).

Chisti, Y., *Airlift Bioreactors*, Elsevier, New York (1989).

Chisti, Y., "Pneumatically Agitated Bioreactors in Industrial and Environmental Bioprocessing: Hydrodynamics, Hydraulics and Transport Phenomena," *Appl. Mech. Rev.*, **51**, 33 (1998).

Chisti, Y., "Mass Transfer," *Encyclopedia of Bioprocess Technology: Fermentation, Biocatalysis and Bioseparation*, Vol. 3, M. C. Flickinger, and S. W. Drew, eds., Wiley, New York, p. 1607, (1999a).

Chisti, Y., "Shear Sensitivity," *Encyclopedia of Bioprocess Technology: Fermentation, Biocatalysis, and Bioseparation*, Vol. 5, M. C. Flickinger, and S. W. Drew, eds., Wiley, New York, p. 2379 (1999b).

Clift, R., J. R. Grace, and M. E. Weber, *Bubbles, Drops, and Particles*, Academic Press, New York (1978).

Contreras, A., F. García, E. Molina, and J. C. Merchuk, "Interaction Between CO_2-Mass Transfer, Light Availability, and Hydrodynamic Stress in the Growth of *Phaeodactylum tricornutum* in a Concentric Tube Airlift Photobioreactor," *Biotechnol. Bioeng.*, **60**, 318 (1998a).

Contreras, A., Y. Chisti, and E. Molina, "A Reassessment of Relationship Between Riser and Downcomer Gas Holdups in Airlift Reactors," *Chem. Eng. Sci.*, **53**, 4151 (1998b).

Deckwer, W.-D., *Bubble Column Reactors*, Wiley, New York (1992).

Ganzeveld, K. J., Y. Chisti, and M. Moo-Young, "Hydrodynamic Behaviour of Animal Cell Microcarrier Suspensions in Split-Cylinder Airlift Bioreactors," *Bioprocess Eng.*, **12**, 239 (1995).

García Camacho, F., A. Contreras Gómez, F. G. Acién Fernández, J. Fernández Sevilla, and E. Molina Grima, "Use of Concentric-Tube Airlift Photobioreactors for Microalgal Outdoor Mass Cultures," *Enzyme Microbial. Technol.*, **24**, 164 (1999).

Hikita, H., S. Asai, K. Tanigawa, K. Segawa, and M. Kitao, "The Volumetric Liquid-Phase Mass Transfer Coefficient in Bubble Columns," *Chem. Eng. J.*, **22**, 61 (1981).

Heijnen, J. J., and K. Van't Riet, "Mass Transfer, Mixing and Heat Transfer Phenomena in Low Viscosity Bubble Column Reactors," *Chem. Eng. J.*, **28**, B21 (1984).

Joshi, J. B., V. V. Ranade, S. D. Gharat, and S. S. Lele, "Sparged Loop Reactors," *Can. J. Chem. Eng.*, **68**, 705 (1990).

Kawase, Y., M. Tsujimura, and T. Yamaguchi, "Gas Hold-Up in External-Loop Airlift Bioreactors," *Bioprocess Eng.*, **12**, 21 (1995).

Lübbert, A., and B. Larson, "Detailed Investigations of the Multiphase Flow in Airlift Tower Loop Reactors," *Chem. Eng. Sci.*, **45**, 3047 (1990).

Lübbert, A., B. Larson, L. W. Wan, and S. Bröring, "Local Mixing Behaviour of Airlift Multiphase Chemical Reactors," *Inst. Chem. Eng.*, Symp. Ser., Vol. 121, p. 203 (1990).

Matthijs, H. C. P., H. Balke, U. M. Van Hes, B. M. A. Kroon, L. R. Mur, and R. A. Binot, "Application of Light-Emitting Diodes in Bioreactors: Flashing Light Effects and Energy Economy in Algal Culture (*Chlorella pyrenoidosa*)," *Biotechnol. Bioeng.*, **50**, 98 (1996).

Merchuk, J. C., and M. Gluz, "Bioreactors, Air-Lift Reactors," *Encyclopedia of Bioprocess Technology: Fermentation, Biocatalysis and Bioseparation*, Vol. 1, M. C. Flickinger, and S. W. Drew, eds., Wiley, New York, p. 320 (1999).

Miyahara, T., M. Hamaguchi, Y. Sukeda, and T. Takehashi, "Size of Bubbles and Liquid Circulation in a Bubble Column with Draught Tube and Sieve Plate," *Can. J. Chem. Eng.*, **64**, 718 (1986).

Okada, K., S. Shibano, and Y. Akagi, "Turbulent Properties in Bubble-Flow Region in External-Loop Airlift Bubble Column," *J. Chem. Eng. Jpn.*, **26**, 637 (1993).

Sánchez Mirón, A., A. Contreras Gómez, F. García Camacho, E. Molina Grima, and Y. Chisti, "Comparative Evaluation of Compact Photobioreactors for Large-Scale Monoculture of Microalgae," *J. Biotechnol.*, **70**, 251 (1999).

Silva, H. J., T. Cortiñas, and R. J. Ertola, "Effect of Hydrodynamic Stress on *Dunaliella* Growth," *J. Chem. Technol. Biotechnol.*, **40**, 41 (1987).

Snoeyink, V. L., and D. Jenkins, *Water Chemistry*, Wiley, New York (1980).
Suzuki, T., T. Matsuo, K. Ohtaguchi, and K. Koide, ''Gas-Sparged Bioreactors for CO_2 Fixation by *Dunaliella tertiolecta*,'' *J. Chem. Technol. Biotechnol.*, **62**, 351 (1995).
Tredici, M. R., ''Bioreactors, Photo,'' *Encyclopedia of Bioprocess Technology*: *Fermentation, Biocatalysis and Bioseparation*, Vol. 1, M. C. Flickinger, and S. W. Drew. Eds, Wiley, New York, p. 395 (1999).
Wenge, F., Y. Chisti, and M. Moo-Young, ''Split-Cylinder Airlift Reactors: Hydraulics and Hydrodynamics of a New Mode of Operation,'' *Chem. Eng. Commun.*, **155**, 19 (1996).

Manuscript received Nov. 8, 1999, and revision received Apr. 13, 2000.